Cavity-Funneled Generation of Indistinguishable Single Photons from Strongly Dissipative Quantum Emitters

Thomas Grange,[1,2,*] Gaston Hornecker,[1,2,3] David Hunger,[4] Jean-Philippe Poizat,[1,2] Jean-Michel Gérard,[1,3] Pascale Senellart,[5] and Alexia Auffèves[1,2]

[1]*Université Grenoble-Alpes, "Nanophysics and Semiconductors" joint team, 38000 Grenoble, France*
[2]*CNRS, Institut Néel, "Nanophysics and Semiconductors" joint team, 38000 Grenoble, France*
[3]*CEA, INAC-SP2M, "Nanophysics and Semiconductors" joint team, 38000 Grenoble, France*
[4]*Fakultät für Physik, Ludwig-Maximilians-Universität, Schellingstrasse 4, 80799 München, Germany*
[5]*CNRS, Laboratoire de Photonique et de Nanostructures, 91460 Marcoussis, France*

(Received 5 February 2015; published 11 May 2015)

We investigate theoretically the generation of indistinguishable single photons from a strongly dissipative quantum system placed inside an optical cavity. The degree of indistinguishability of photons emitted by the cavity is calculated as a function of the emitter-cavity coupling strength and the cavity linewidth. For a quantum emitter subject to strong pure dephasing, our calculations reveal that an unconventional regime of high indistinguishability can be reached for moderate emitter-cavity coupling strengths and high-quality factor cavities. In this regime, the broad spectrum of the dissipative quantum system is funneled into the narrow line shape of the cavity. The associated efficiency is found to greatly surpass spectral filtering effects. Our findings open the path towards on-chip scalable indistinguishable-photon-emitting devices operating at room temperature.

DOI: 10.1103/PhysRevLett.114.193601 PACS numbers: 42.50.Pq, 03.65.Yz, 42.50.Ct, 78.67.-n

Indistinguishable single photons are the building blocks of various optically based quantum information applications such as linear optical quantum computing [1,2], boson sampling [3–7], quantum teleportation [8], or quantum networks [9]. Indistinguishable photons are usually generated either by using parametric down-conversion [10] or, alternatively, directly from a single two-level quantum emitter such as atoms, color centers, quantum dots, or organic molecules [11–20]. Parametric down-conversion is presently the most mature technology available, but the usual low efficiency of the nonlinear processes is a severe limitation to the scalability of such sources. On the other hand, sources based on single solid-state quantum systems have been greatly developed in the past decade, as they hold the promise to combine indistinguishable, on-demand, energy-efficient, electrically drivable, and scalable characteristics. However, except at cryogenics temperature, solid-state systems emitting single photons are subject to strong pure dephasing processes [21–29], making them at first view inappropriate for quantum applications requiring photon indistinguishability.

A two-level quantum emitter (QE) coupled only to vacuum fluctuations should emit perfectly indistinguishable photons. However, as soon as pure dephasing of the QE occurs, the degree of indistinguishability of the emitted photons is reduced to [30]

$$I = \frac{\gamma}{\gamma + \gamma^*} = \frac{T_2}{2T_1}, \tag{1}$$

where $\gamma = 1/T_1$ is the population decay rate, $\gamma^*/2 = 1/T_2^*$ the pure dephasing rate, and $1/T_2 = 2/T_1 + 1/T_{2*}$ the total dephasing rate. For solid-state QE-emitting photons at room temperature such as color centers, quantum dots, or organic molecules, pure dephasing rates are typically several orders of magnitude larger than the population decay rate (typically ranging from 3 to 6 orders of magnitude) [12,14,21,22,24,26–29,31]. Hence, the intrinsic indistinguishability given by Eq. (1) is almost zero. A possible way to enhance the indistinguishability is to spectrally filter the emitted photons *a posteriori*. However, this linear-filter strategy leads to a very low efficiency. Engineering of both efficiency and indistinguishability are possible by placing the dissipative QE in an optical cavity [15,27,32–44]. A usual strategy is then to use the Purcell effect to enhance the spontaneous emission, as in Eq. (1) an increase in γ results in an increase of I. However, reaching Purcell factors larger than γ^*/γ for room-temperature solid-state systems appears to be well beyond the present experimental state of the art.

In this Letter, we propose a realistic and robust way to generate highly indistinguishable photons from strongly dissipative QE (i.e., for $\gamma^* \gg \gamma$). The idea is to exploit a cavity-quantum-electrodynamics (cavity-QED) regime of low cavity linewidth and moderate cavity-emitter coupling, in which the broad spectrum of the dissipative QE is funneled into the narrow emission line of the cavity. In this regime, high indistinguishability is predicted together with efficiencies orders of magnitude higher than spectral filtering. Insights into the full quantum calculation are gained by semiclassical derivations of indistinguishability in limiting cases of dissipative cavity QED.

As depicted in Fig. 1, we consider a two-level QE system $\{|\psi_g\rangle, |\psi_e\rangle\}$ coupled to a cavity mode whose Fock states are denoted $\{|0\rangle, |1\rangle, \ldots\}$. All the dissipative terms are assumed to be described within the Markov approximation [45,46]. The relevant parameters are the QE decay rate γ (which may include radiative as well as nonradiative components), the cavity decay rate κ, and the pure dephasing rate γ^*; g is the dipolar coupling between the QE and the cavity mode (see Fig. 1). The emitter-cavity detuning is set to zero (i.e., perfect resonance). For simplicity, we assume an instantaneous excitation of the QE, so that only one quantum of excitation can be transferred to the cavity. Within the rotating-wave approximation, it is therefore sufficient to investigate the dissipative quantum dynamics in the two-dimensional Hilbert space formed by $\{|\psi_e, 0\rangle, |\psi_g, 1\rangle\}$. The degree of indistinguishability of photons can be defined by the probability of two-photon interference in a Hong-Ou-Mandel experiment [47]. For a single-photon emitter, this indistinguishability figure of merit reads [30,43,48,49]

$$I = \frac{\int_0^\infty dt \int_0^\infty d\tau |\langle \hat{a}^\dagger(t+\tau)\hat{a}(t)\rangle|^2}{\int_0^\infty dt \int_0^\infty d\tau \langle \hat{a}^\dagger(t)\hat{a}(t)\rangle \langle \hat{a}^\dagger(t+\tau)\hat{a}(t+\tau)\rangle}, \quad (2)$$

where $a^{(\dagger)}$ are the ladder operators of the electromagnetic (EM) mode in which the photons are emitted. This equation imposes the necessary condition for perfectly indistinguishable photons that time correlations of the EM field decay the same way as the intensity, i.e., that photons are Fourier-transform limited. The calculation of the above quantities can be separated into two steps (see Supplemental Material [49]). First, we calculate the evolution of the density matrix $\hat{\rho}(t)$ by solving the Lindblad equation:

$$\hat{\rho}(t) = e^{-i\hat{\mathcal{L}}t}|\psi_e, 0\rangle\langle\psi_e, 0|, \quad (3)$$

where $\hat{\mathcal{L}}$ is the total Liouvillian of the system [49]. Second, we calculate the retarded Green's function, which reads in the $\{|\psi_e, 0\rangle, |\psi_g, 1\rangle\}$ basis

$$\hat{G}^R(\omega) = \begin{pmatrix} \omega + i\gamma/2 + i\gamma^*/2 & g \\ g & \omega - \delta + i\kappa/2 \end{pmatrix}^{-1}. \quad (4)$$

The two-time correlator of the cavity field can be expressed as a product of the retarded propagator $\hat{G}^R(\tau) = -i\int d\omega e^{-i\omega t}\hat{G}^R(\omega)$ and the density matrix [49]:

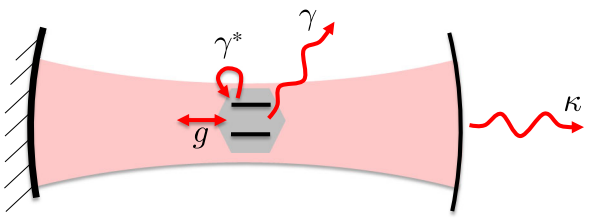

FIG. 1 (color online). Schematic of the system under study: a dissipative two-level emitter coupled to an optical-cavity mode.

$$\langle a^\dagger(t+\tau)a(t)\rangle = \langle \psi_g, 1|\hat{G}^R(\tau)\hat{\rho}(t)|\psi_g, 1\rangle. \quad (5)$$

In Fig. 2, we report calculations for strongly dissipative emitters verifying $\gamma^* = 10^4\gamma$. This is a typical value for a solid-state QE at room temperature, and the results are qualitatively similar for any strongly dissipative emitters verifying $\gamma^* \gg \gamma$. Without any cavity, the degree of indistinguishability would then amount to 10^{-4} according to Eq. (1). In Fig. 2(a), I is plotted as a function of the coupling g and the cavity linewidth κ, while γ and γ^* are fixed. Two regions of high indistinguishability are found, which are discussed below. The one in the upper-right corner corresponds to very large couplings g and broad cavities such as $g > \gamma^*$ and $\kappa > \gamma^*$, which is extremely challenging to reach experimentally for strongly dissipative emitters (i.e., for large values of γ^*). The other region of high indistinguishability, in the lower-left corner, appears for good cavities for $\kappa < \gamma$ together with moderate or small coupling values g. As these values are within experimental reach, this unconventional regime is highly attractive for the generation of indistinguishable photons.

To get a physical insight into the calculated indistinguishability, we divide the (κ,g) space into three regimes labeled from 1 to 3 in Fig. 2 and study the corresponding limiting cases below. First, we can distinguish between the QE-cavity coherent regime occurring for $2g > \kappa + \gamma + \gamma^*$ and the incoherent regime $2g < \kappa + \gamma + \gamma^*$. In the coherent regime, labeled 1 in Fig. 2, the dynamics consists of damped Rabi oscillations which evolves into an incoherent population of the two polariton modes (i.e., mixed QE-cavity state). In the limit where $2g \gg \kappa + \gamma + \gamma^*$, the indistinguishability degree reads [49]

$$I_{cc} = \frac{(\gamma+\kappa)(\gamma+\kappa+\gamma^*/2)}{(\gamma+\kappa+\gamma^*)^2}. \quad (6)$$

As this expression is independent of g, increasing g alone does not allow us to reach arbitrarily large indistinguishability, as seen in Fig. 2. On the contrary, nearly perfect indistinguishability occurs in the coherent regime only if $2g \geq \kappa \gg \gamma^*$.

In the incoherent limit ($2g \ll \kappa + \gamma + \gamma^*$), the dynamics of the system can be described in terms of incoherent population transfer with an effective transfer rate between the QE and the cavity given by [45,46]

$$R = \frac{4g^2}{\kappa + \gamma + \gamma^*}. \quad (7)$$

Within this incoherent regime, we can further define a bad-cavity regime for $\kappa > \gamma + \gamma^*$ (labeled 2 in Fig. 2) and a good-cavity regime for $\kappa < \gamma + \gamma^*$ (labeled 3 in Fig. 2) [45,50]. In the bad-cavity limit $\kappa \gg \gamma + \gamma^*$, the cavity can be adiabatically eliminated, and its sole effect is to add a new channel of irreversible radiative emission at a rate R. Reabsorption by the QE is then negligible. The dynamics of the coupled system can then be described by the one of an

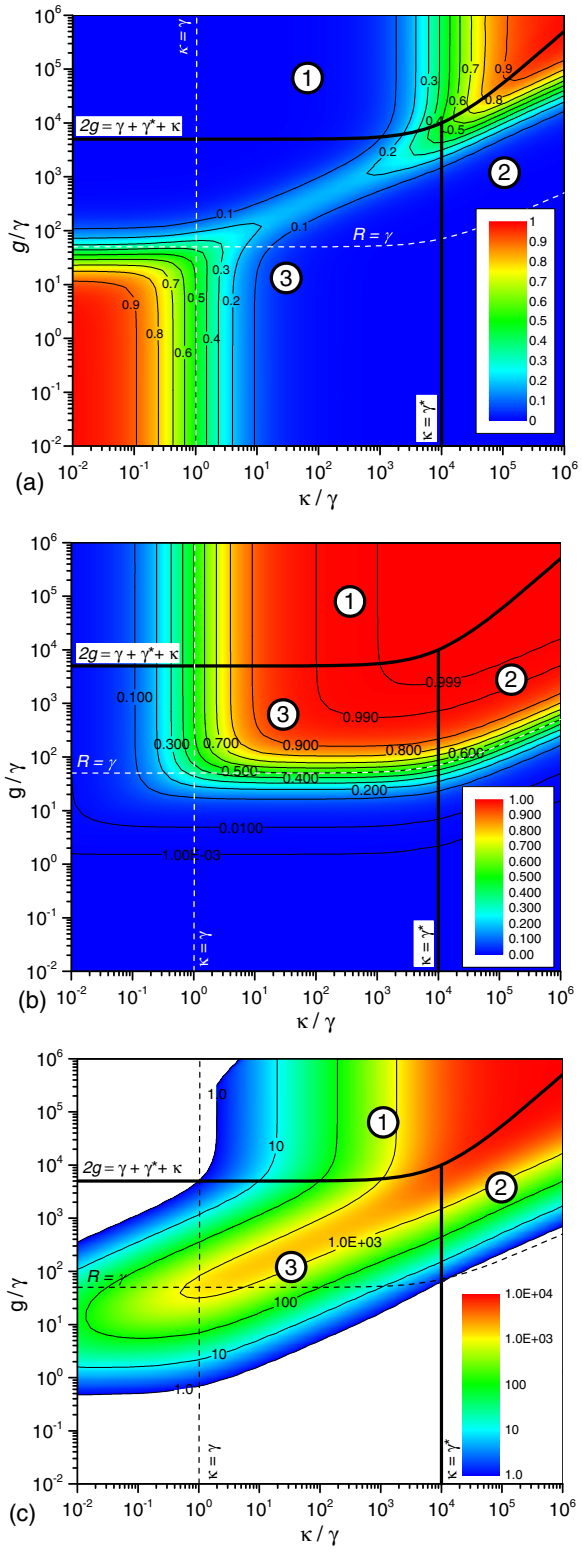

FIG. 2 (color online). (a) Indistinguishability figure of merit (I), (b) efficiency β, and (c) funneling ratio $\mathcal{F}$, plotted as a function of the cavity linewidth κ/γ and the emitter-cavity coupling strength g/γ for a fixed ratio $\gamma^*/\gamma = 10^4$. The funneling ratio is defined as $\mathcal{F} = \beta I \gamma^*/\gamma$. Solid lines delimit three different regimes discussed in the text: coherent coupling ("1"), incoherent coupling and bad-cavity regime ("2"), and incoherent coupling and good-cavity regime ("3").

effective QE with a decay rate $\gamma + R$. Applying Eq. (1) to this effective QE leads to an indistinguishability of

$$I_{bc} = \frac{\gamma + R}{\gamma + R + \gamma^*}. \tag{8}$$

Within this regime of an incoherently coupled bad cavity, the usual strategy to increase indistinguishability is basically to maximize R. This can be done by increasing g and/or minimizing κ. However, from Eq. (8), near-unity indistinguishability requires $R \gg \gamma^*$ and consequently $2g \gg \gamma^*$. It is found that the coupling strength g has to exceed γ^* by nearly one order of magnitude in order to reach an indistinguishability value of $I = 0.9$. Reaching such coupling is technologically extremely challenging for solid-state emitters under ambient temperature.

On the other hand, the incoherent good-cavity regime (labeled 3 in Fig. 2) occurs for $\kappa < \gamma + \gamma^*$. In this regime, the cavity can store the photons within a time scale comparable to or longer than the QE dephasing time. The cavity itself then acts as an effective emitter incoherently pumped by the QE [49], so that the cavity field correlations read

$$\langle a^\dagger(t+\tau)a(t)\rangle = \rho_{cc}(t)e^{-\Gamma_c \tau/2}, \tag{9}$$

where $\rho_{cc}(t)$ is the population of the cavity mode and Γ_c is the linewidth of the cavitylike eigenstate. From Eq. (4), one can derive that $\Gamma_c = \kappa + R$, which is the sum of the cavity decay rate κ into EM modes plus the incoherent reabsorption rate R between the cavity and the QE. By solving the population rate equations and by plugging in the resulting cavity dynamics $\rho_{cc}(t)$ in Eqs. (9) and (2), one finds an indistinguishability of [49]

$$I_{gc} = \frac{\gamma + \frac{\kappa R}{\kappa + R}}{\gamma + \kappa + 2R}. \tag{10}$$

Consequently, large indistinguishability occurs in this regime for $\kappa < \gamma$ and $R < \gamma$ (i.e., $g < \sqrt{\gamma\gamma^*}/2$), in agreement with the full calculation shown in Fig. 2(a). This can be understood by noting that two ingredients are involved in the degradation of indistinguishability in this good-cavity regime where the cavity acts as the effective emitter. The first point is that the initial incoherent feeding of the cavity occurs on a time scale $1/\gamma$, producing a time uncertainty in the population of the cavity. Hence, κ has to be kept small compared to γ in order to prevent such a time-jittering effect, in analogy to the incoherent pumping of QE via high energy states [48]. The second point is that, after the initial filling of the cavity, incoherent exchange processes between the QE and the cavity can still occur. However, back and forth incoherent hopping between the cavity and the QE leads to the dephasing of the photons emitted by the cavity. To prevent such detrimental hopping, $R < \gamma$ is required.

We now discuss the efficiency of the photon emission from the cavity mode, i.e., the probability to have emission by the cavity mode per initial excitation of the QE. The efficiency of photon emission in the cavity mode is given by

$$\beta = \kappa \int_0^\infty \langle a^\dagger(t) a(t) \rangle. \tag{11}$$

In Fig. 2(b), the efficiency β is plotted as a function of the cavity linewidth κ and the emitter-cavity coupling strength g. Near-unitary (i.e., on-demand) efficiencies are obtained in the upper-right corner. In the weak-coupling regime, we find

$$\beta = \frac{\kappa R}{\kappa R + \gamma(\kappa + R)}. \tag{12}$$

Efficiencies larger than 0.5 are typically obtained for $R > \gamma$ and $\kappa > R$. This is compatible with high indistinguishability in the region of high g and high κ values (i.e., upper-right corner in Fig. 2) but not in the good-cavity regime (i.e., region 3 in Fig. 2). Nevertheless, as discussed in the following, the product of efficiency and indistinguishability βI in the good-cavity regime can still be way above the one obtained by any linear spectral filtering technique. Let us consider a linear spectral filter, with a narrow spectral range $\Delta\nu_f$, through which the spectrum of the broad QE is sent. We assume $\Delta\nu_f \ll \gamma^*$. The output efficiency is bounded by $\beta_f \leq \Delta\nu_f/\gamma^*$. Because of the Fourier-transform condition, the corresponding indistinguishability is bounded by $I_f \leq \gamma/\Delta\nu_f$. Hence the efficiency-indistinguishability product for spectral filtering cannot exceed $\beta_f I_f \leq \gamma/\gamma^*$. In order to compare $\beta \times I$ in the present cavity-QED scheme with the upper limit for spectral filtering, we define a cavity-funneling factor

$$\mathcal{F} = \frac{\gamma^*}{\gamma} \beta I, \tag{13}$$

such that $\mathcal{F}$ values larger than unity necessarily indicate a spectral cavity-funneling effect. $\mathcal{F}$ indicates the minimum enhancement ratio of $\beta \times I$ with respect to any spectral-filtering effect. In practice, this enhancement will be larger, since light emitted from a cavity can be very efficiently collected [15], in contrast to free-space spontaneous emission. In Fig. 2(c), the funneling $\mathcal{F}$ is plotted in the same parameter range (κ,g) as previous plots. Only the values satisfying the cavity-funneling condition of $\mathcal{F} > 1$ are shown. It appears clearly that almost-perfect indistinguishability in the good-cavity regime is compatible with cavity funneling. In Fig. 3, I, β, and $\mathcal{F}$ are plotted as a function of κ for a fixed value of g. The full calculation is found to be in good agreement with the above formulas for the incoherent regime. It illustrates the necessary trade-off between indistinguishability and efficiency in the good-cavity regime, where a clear maximum of the funneling factor occurs. The large calculated values for $\mathcal{F}$ are signatures of a very efficient redirection of the QE spectrum into the unperturbed cavity spectrum of linewidth κ.

Finally, we argue that exploiting this unconventional cavity-QED regime is a promising way for efficiently generating indistinguishable single photons from solid-state

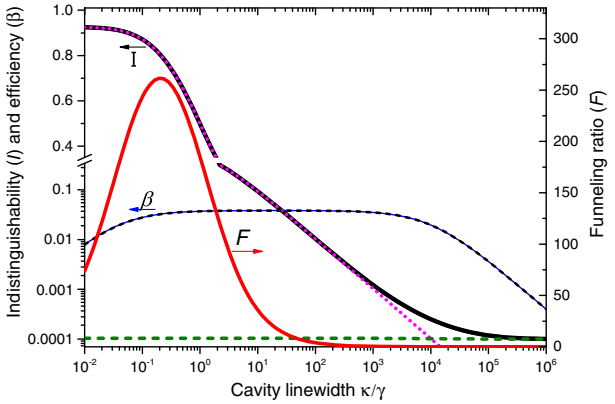

FIG. 3 (color online). Indistinguishability figure of merit I (full calculation in black solid line), efficiency β (blue solid line), and cavity-funneling ratio $\mathcal{F}$ (red solid line) for a fixed emitter-cavity coupling of $g = 10\gamma$. The full calculation for indistinguishability is compared with analytic expressions in two different limiting cases: incoherently coupled good-cavity regime [dotted line, Eq. (10)] and coherently coupled bad-cavity regime [dashed line, Eq. (8)]. The analytical expression for β [dotted line, Eq. (12)] overlaps perfectly with the full calculation.

QEs at room temperature. To illustrate this general strategy, we propose below two possible implementations. We first consider a single self-assembled quantum dot coupled to a photonic crystal cavity. State-of-the-art photonic crystal cavities can provide $\hbar g = 120$ μeV and $\hbar\kappa = 20$ μeV [51]. Assuming $\hbar\gamma = 60$ μeV and $\hbar\gamma^* = 7$ meV for an InAs/GaAs quantum dot at 300 K [21,52,53], we predict $I = 0.72$, $\beta = 0.088$, and $\mathcal{F} = 7.3$. Second, we consider a single silicon vacancy (SiV) center in a nanodiamond coupled to a fiber cavity. For SiV at 300 K, we take $\gamma = 2\pi \times 160$ MHz and $\gamma^* = 2\pi \times 550$ GHz [54]. Coupling SiV with a fiber cavity with $g = 2\pi \times 1.0$ GHz and $\kappa = 2\pi \times 30$ MHz is within experimental reach [39], for which our calculation predicts $I = 0.81$, $\beta = 0.035$, and $\mathcal{F} = 99$. These predicted degrees of indistinguishability at room temperature, which are comparable with state-of-the-art values obtained from low-temperature single-photon sources under incoherent pumping [15], allow various applications in quantum information such as the production of entangled photon pairs through the use of CNOT gates [55].

In summary, for strongly dissipative emitters we predict an unconventional regime of high indistinguishability in which the broad spectrum of the quantum emitter is funneled into a narrow cavity resonance. For typical room-temperature quantum emitters, the associated efficiency can surpass any spectral filtering schemes by orders of magnitude. This strategy opens the road towards the generation of indistinguishable single photons from solid-state quantum emitters under ambient temperature.

This work has been funded by the European Union's Seventh Framework Programme (FP7) under Grant Agreement No. 618078 (WASPS). Jason Smith and John Rarity are acknowledged for fruitful discussions.

*thomas.grange@neel.cnrs.fr

[1] E. Knill, R. Laflamme, and G. J. Milburn, Nature (London) **409**, 46 (2001).
[2] P. Kok, W. J. Munro, K. Nemoto, T. C. Ralph, J. P. Dowling, and G. Milburn, Rev. Mod. Phys. **79**, 135 (2007).
[3] J. B. Spring *et al.*, Science **339**, 798 (2013).
[4] M. A. Broome, A. Fedrizzi, S. Rahimi-Keshari, J. Dove, S. Aaronson, T. C. Ralph, and A. G. White, Science **339**, 794 (2013).
[5] A. Crespi, R. Osellame, R. Ramponi, D. J. Brod, E. F. Galvão, N. Spagnolo, C. Vitelli, E. Maiorino, P. Mataloni, and F. Sciarrino, Nat. Photonics **7**, 545 (2013).
[6] M. Tillmann, B. Dakić, R. Heilmann, S. Nolte, A. Szameit, and P. Walther, Nat. Photonics **7**, 540 (2013).
[7] N. Spagnolo *et al.*, Nat. Photonics **8**, 615 (2014).
[8] D. Fattal, E. Diamanti, K. Inoue, and Y. Yamamoto, Phys. Rev. Lett. **92**, 037904 (2004).
[9] H. Kimble, Nature (London) **453**, 1023 (2008).
[10] M. Eisaman, J. Fan, A. Migdall, and S. Polyakov, Rev. Sci. Instrum. **82**, 071101 (2011).
[11] C. Santori, D. Fattal, J. Vučković, G. S. Solomon, and Y. Yamamoto, Nature (London) **419**, 594 (2002).
[12] A. Kiraz, M. Ehrl, T. Hellerer, Ö. Müstecaplıoğlu, C. Bräuchle, and A. Zumbusch, Phys. Rev. Lett. **94**, 223602 (2005).
[13] R. B. Patel, A. J. Bennett, I. Farrer, C. A. Nicoll, D. A. Ritchie, and A. J. Shields, Nat. Photonics **4**, 632 (2010).
[14] R. Lettow, Y. Rezus, A. Renn, G. Zumofen, E. Ikonen, S. Götzinger, and V. Sandoghdar, Phys. Rev. Lett. **104**, 123605 (2010).
[15] O. Gazzano, S. M. de Vasconcellos, C. Arnold, A. Nowak, E. Galopin, I. Sagnes, L. Lanco, A. Lemaître, and P. Senellart, Nat. Commun. **4**, 1425 (2013).
[16] Y.-M. He, Y. He, Y.-J. Wei, D. Wu, M. Atatüre, C. Schneider, S. Höfling, M. Kamp, C.-Y. Lu, and J.-W. Pan, Nat. Nanotechnol. **8**, 213 (2013).
[17] M. Müller, S. Bounouar, K. D. Jöns, M. Glässl, and P. Michler, Nat. Photonics **8**, 224 (2014).
[18] L. Monniello, A. Reigue, R. Hostein, A. Lemaître, A. Martinez, R. Grousson, and V. Voliotis, Phys. Rev. B **90**, 041303 (2014).
[19] A. Sipahigil, K. D. Jahnke, L. J. Rogers, T. Teraji, J. Isoya, A. S. Zibrov, F. Jelezko, and M. D. Lukin, Phys. Rev. Lett. **113**, 113602 (2014).
[20] Y.-J. Wei *et al.*, Nano Lett. **14**, 6515 (2014).
[21] P. Borri, W. Langbein, S. Schneider, U. Woggon, R. L. Sellin, D. Ouyang, and D. Bimberg, Phys. Rev. Lett. **87**, 157401 (2001).
[22] M. Bayer and A. Forchel, Phys. Rev. B **65**, 041308 (2002).
[23] A. Berthelot, I. Favero, G. Cassabois, C. Voisin, C. Delalande, P. Roussignol, R. Ferreira, and J.-M. Gérard, Nat. Phys. **2**, 759 (2006).
[24] S. Kako, C. Santori, K. Hoshino, S. Götzinger, Y. Yamamoto, and Y. Arakawa, Nat. Mater. **5**, 887 (2006).
[25] T. Grange, Phys. Rev. B **80**, 245310 (2009).
[26] S. Bounouar *et al.*, Nano Lett. **12**, 2977 (2012).
[27] R. Albrecht, A. Bommer, C. Deutsch, J. Reichel, and C. Becher, Phys. Rev. Lett. **110**, 243602 (2013).
[28] R. Albrecht, A. Bommer, C. Pauly, F. Mücklich, A. W. Schell, P. Engel, T. Schröder, O. Benson, J. Reichel, and C. Becher, Appl. Phys. Lett. **105**, 073113 (2014).
[29] L. J. Rogers *et al.*, Nat. Commun. **5**, 5739 (2014).
[30] J. Bylander, I. Robert-Philip, and I. Abram, Eur. Phys. J. D **22**, 295 (2003).
[31] B. Lounis and W. Moerner, Nature (London) **407**, 491 (2000).
[32] J.-M. Gérard, B. Sermage, B. Gayral, B. Legrand, E. Costard, and V. Thierry-Mieg, Phys. Rev. Lett. **81**, 1110 (1998).
[33] L. C. Andreani, G. Panzarini, and J.-M. Gérard, Phys. Rev. B **60**, 13276 (1999).
[34] E. Moreau, I. Robert, J.-M. Gérard, I. Abram, L. Manin, and V. Thierry-Mieg, Appl. Phys. Lett. **79**, 2865 (2001).
[35] J. Reithmaier, G. Sek, A. Löffler, C. Hofmann, S. Kuhn, S. Reitzenstein, L. Keldysh, V. Kulakovskii, T. Reinecke, and A. Forchel, Nature (London) **432**, 197 (2004).
[36] S. Varoutsis, S. Laurent, P. Kramper, A. Lemaître, I. Sagnes, I. Robert-Philip, and I. Abram, Phys. Rev. B **72**, 041303 (2005).
[37] K. Hennessy, A. Badolato, M. Winger, D. Gerace, M. Atatüre, S. Gulde, S. Fält, E. L. Hu, and A. Imamoğlu, Nature (London) **445**, 896 (2007).
[38] Z. Di, H. V. Jones, P. R. Dolan, S. M. Fairclough, M. B. Wincott, J. Fill, G. M. Hughes, and J. M. Smith, New J. Phys. **14**, 103048 (2012).
[39] H. Kaupp, C. Deutsch, H.-C. Chang, J. Reichel, T. W. Hänsch, and D. Hunger, Phys. Rev. A **88**, 053812 (2013).
[40] J. Riedrich-Moller, C. Arend, C. Pauly, F. Mucklich, M. Fischer, S. Gsell, M. Schreck, and C. Becher, Nano Lett. **14**, 5281 (2014).
[41] P. Pathak and S. Hughes, Phys. Rev. B **82**, 045308 (2010).
[42] T. Close, E. M. Gauger, and B. W. Lovett, New J. Phys. **14**, 113004 (2012).
[43] P. Kaer, P. Lodahl, A.-P. Jauho, and J. Mørk, Phys. Rev. B **87**, 081308 (2013).
[44] P. Kaer and J. Mørk, Phys. Rev. B **90**, 035312 (2014).
[45] A. Auffèves, J.-M. Gérard, and J.-P. Poizat, Phys. Rev. A **79**, 053838 (2009).
[46] A. Auffèves, D. Gerace, J.-M. Gérard, M. F. Santos, L. Andreani, and J.-P. Poizat, Phys. Rev. B **81**, 245419 (2010).
[47] C. Hong, Z. Ou, and L. Mandel, Phys. Rev. Lett. **59**, 2044 (1987).
[48] A. Kiraz, M. Atatüre, and A. Imamoğlu, Phys. Rev. A **69**, 032305 (2004).
[49] See Supplemental Material at http://link.aps.org/supplemental/10.1103/PhysRevLett.114.193601 for details on the theory.
[50] A. Auffèves, B. Besga, J.-M. Gérard, and J.-P. Poizat, Phys. Rev. A **77**, 063833 (2008).
[51] Y. Arakawa, S. Iwamoto, M. Nomura, A. Tandaechanurat, and Y. Ota, IEEE J. Sel. Top. Quantum Electron. **18**, 1818 (2012).
[52] R. Heitz, I. Mukhametzhanov, A. Madhukar, A. Hoffmann, and D. Bimberg, J. Electron. Mater. **28**, 520 (1999).
[53] The line shape of self-assembled quantum dots at room temperature can be approximated by Lorentzians, as at such high temperature Markovian pure dephasing effects dominates over non-Markovian phonon sideband effects [21].
[54] E. Neu, D. Steinmetz, J. Riedrich-Möller, S. Gsell, M. Fischer, M. Schreck, and C. Becher, New J. Phys. **13**, 025012 (2011).
[55] O. Gazzano, M. Almeida, A. Nowak, S. Portalupi, A. Lemaître, I. Sagnes, A. White, and P. Senellart, Phys. Rev. Lett. **110**, 250501 (2013).